Supporting Information

Borghi et al. 10.1073/pnas.1204390109

SI Materials and Methods

Constructs. The EcadTSMod construct was assembled (Epoch Life Science) from canine E-cadherin cDNA (1) and the TSMod sequence (2). TSMod was flanked with linkers GGAGGAGCAGGAGCAGGC upstream and GGAGGAGCAGGAGCAGGA downstream and inserted between V742 and K743 of E-cadherin, which are the fourth and fifth residues of the juxtamembrane domain, respectively. The EcadTSModΔcyto construct was assembled from E-cadherin residues 1–768 appended with the TSMod sequence. The mutations K743R, L746V, and L747A within the juxtamembrane domain were included to ensure targeting of the construct to the plasma membrane and cell–cell contacts despite the lack of catenin binding sites (3).

FRET calibration constructs mTFP-TRAF-Venus and mTFP-5aa-Venus were obtained from R. N. Day [Indiana University, Indianapolis, IN (4)]. Bleed-through values used for correcting FRET intensities were collected using EcadTSModΔmTFP and EcadTSModΔVenus constructs, generated (Epoch Life Science) from the EcadTSMod construct in which either mTFP or Venus was deleted between the flagelliform polypeptide of the TSMod sequence and the upstream or downstream flanking linker, respectively.

Cells. Cells were maintained in low (MDCK G type II) or high (L cells) glucose Dulbecco's modified Eagle medium (DMEM) containing 1 g/L sodium bicarbonate and supplemented with 10% (vol/vol) FBS, penicillin, streptomycin, and kanamycin as described previously (5, 6). TSMod-tagged constructs were transfected using Lipofectamine 2000 (MDCK cells) or Lipofectamine LTX (L cells) according to the instructions of the manufacturer (Invitrogen). Cell-stretching experiments (see Fig. 4) used a MDCK cell line stably expressing the EcadTSMod construct that was obtained by selection with G418. Before live-cell observation or fixation, cells were washed and trypsinized in PBS, seeded on collagen-coated surfaces, and allowed to adhere overnight.

RNA Interference and Pharmacological Perturbations. Canine αE-catenin depletion was obtained by short shRNA interference with annealed primers expressed in a pSuper vector [a gift from I. G. Macara, University of Virginia, Charlottesville, VA (7)], cotransfected with the EcadTSMod construct using Lipofectamine 2000 according to the instructions of the manufacturer. Cells were used for experiments between 48 and 72 h after transfection. In these conditions, more than 90% of cotransfected cells had a decrease of ∼90% in αE-catenin content, as shown previously (8).

Cytochalasin B was used at a final concentration of 10 μM from a stock solution of 10 mg/mL in DMSO (Sigma), and ML-7 was used at a final concentration of 25 μM from a stock solution of 10 mg/mL in EtOH:H_2O 1:1 (Sigma), as published previously (9). Experiments were performed within 1 h after drug perfusion.

Micromanipulation. Microneedles were pulled from glass rods (BR-100-10; VWR) using a pipette puller (P-97; Sutter Instruments) to a final diameter between 2 and 20 μm. Microneedles were manipulated with an automated three-axis micromanipulator (Eppendorf; 5170). Cells were pinched between the tip of the microneedle and the coverslip and were stretched in a stepwise fashion by moving the microneedle away in the *x-y* plane. The extension ratio is $L(t)/L_0$, where $L(t)$ is the end-to-end length of the cell of a doublet not in direct contact with the needle along the axis perpendicular to the cell–cell contact of interest at time t, and L_0 is L at rest ($t = 0$).

Immunostaining. Cells were fixed with a solution of 4% paraformaldehyde in PBS plus 500 μM Ca^{2+}, permeabilized with a solution of 0.1% Triton X-100 in PBS, blocked with a solution of 0.2% BSA plus 1% goat and donkey sera in PBS, incubated with anti–αE-catenin antibody (mouse; 15D9; 1:100; Alexis) or anti–β-catenin antibody [custom rabbit polyclonal, 1:500 (10)], then a secondary $F(ab')_2$ goat/donkey anti–mouse/rabbit IgG labeled with rhodamine red-X (1:200; Jackson ImmunoResearch), and finally mounted in Fluoromount G (Southern Biotech).

Fluorescence Microscopy. Fixed and live cells in DMEM without phenol red supplemented with 25 mM Hepes at 37 °C were imaged on a Zeiss Axiovert 200M inverted microscope customized by Intelligent Imaging , as described previously (8). Briefly, epifluorescence excitation was provided by a xenon arc lamp (DG4 300W; Sutter Instruments) with a dual galvanometric filter changer and cells were viewed with a 63× oil objective (Olympus). FRET imaging was performed on live cells using the Semrock FRET-CFP/YFP-B-000 filter set for mTFP and FRET channels and the excitation filter and beam splitter of a Chroma JP4 filter set in combination with the emitter of the Semrock FRET-CFP/YFP-B-000 filter set for the Venus channel. Images were acquired with a CoolSNAP HQ camera (Roper Scientific), and the system was controlled with Slidebook software. Exposure time was identical for all three channels.

FRET Analysis. Fluorescent images were analyzed in Image J using the Fiji distribution (http://fiji.sc/wiki/index.php/Fiji) and the publicly available PixFRET plugin [http://www.unil.ch/cig/page16989.html (11)], and in-house plugins and macros as follows. All channels were background-subtracted, checked for alignment and, when necessary, registered by no more than 1 pixel. The raw fluorescence intensity from the FRET channel ($I_{\text{raw FRET}}$) was corrected for spectral bleed-through pixel by pixel to yield the corrected FRET intensity $I_{\text{FRET}} = I_{\text{raw FRET}} - \text{BT}_{\text{donor}} \times I_{\text{mTFP}} - \text{BT}_{\text{acceptor}} \times I_{\text{Venus}}$, where I_{mTFP} and I_{Venus} are the fluorescence intensities of the subscript channels and intensity-independent donor and acceptor bleed-throughs were $\text{BT}_{\text{donor}} = 47\%$ and $\text{BT}_{\text{acceptor}} = 18\%$, respectively, as measured with the bleed-through correction constructs mentioned above. The FRET index was computed as $I_{\text{FRET}}/(I_{\text{mTFP}} + I_{\text{FRET}})$. Manual intensity thresholding of the Venus channel was used to segment the cell–cell contact regions and the free membrane regions out from the cells and the background, respectively. FRET index was then averaged over the segmented cell–cell contacts and over the contact-free membrane regions.

FRET index to FRET efficiency calibration was performed with mTFP-TRAF-Venus and mTFP-5aa-Venus constructs. The measured FRET index values (Fig. S2) were paired to previously published FRET efficiency values for those constructs (on our system, a FRET index of 50% for mTFP-5aa-Venus corresponds to 55% FRET efficiency, and a FRET index of 16% for mTFP-TRAF-Venus corresponds to 11% FRET efficiency (table 2 in ref. 4). Linear interpolation between those values was used to infer FRET efficiencies from all other FRET index measurements in our experiments. Forces were subsequently obtained from previously published calibration of FRET efficiency to Force for TSMod (figure 2i in ref. 2).

1. Adams CL, Chen Y-T, Smith SJ, Nelson WJ (1998) Mechanisms of epithelial cell-cell adhesion and cell compaction revealed by high-resolution tracking of E-cadherin-green fluorescent protein. *J Cell Biol* 142:1105–1119.
2. Grashoff C, et al. (2010) Measuring mechanical tension across vinculin reveals regulation of focal adhesion dynamics. *Nature* 466:263–266.
3. Hong S, Troyanovsky RB, Troyanovsky SM (2010) Spontaneous assembly and active disassembly balance adherens junction homeostasis. *Proc Natl Acad Sci USA* 107: 3528–3533.
4. Day RN, Booker CF, Periasamy A (2008) Characterization of an improved donor fluorescent protein for Forster resonance energy transfer microscopy. *J Biomed Opt* 13:031203.
5. Mays RW, et al. (1995) Hierarchy of mechanisms involved in generating Na/K-ATPase polarity in MDCK epithelial cells. *J Cell Biol* 130:1105–1115.
6. Angres B, Barth A, Nelson WJ (1996) Mechanism for transition from initial to stable cell-cell adhesion: Kinetic analysis of E-cadherin-mediated adhesion using a quantitative adhesion assay. *J Cell Biol* 134:549–557.
7. Capaldo CT, Macara IG (2007) Depletion of E-cadherin disrupts establishment but not maintenance of cell junctions in Madin-Darby canine kidney epithelial cells. *Mol Biol Cell* 18:189–200.
8. Borghi N, Lowndes M, Maruthamuthu V, Gardel ML, Nelson WJ (2010) Regulation of cell motile behavior by crosstalk between cadherin- and integrin-mediated adhesions. *Proc Natl Acad Sci USA* 107:13324–13329.
9. Yamada S, Nelson WJ (2007) Localized zones of Rho and Rac activities drive initiation and expansion of epithelial cell-cell adhesion. *J Cell Biol* 178:517–527.
10. Hinck L, Nelson WJ, Papkoff J (1994) Wnt-1 modulates cell-cell adhesion in mammalian cells by stabilizing beta-catenin binding to the cell adhesion protein cadherin. *J Cell Biol* 124:729–741.
11. Feige JN, Sage D, Wahli W, Desvergne B, Gelman L (2005) PixFRET, an ImageJ plug-in for FRET calculation that can accommodate variations in spectral bleed-throughs. *Microsc Res Tech* 68:51–58.

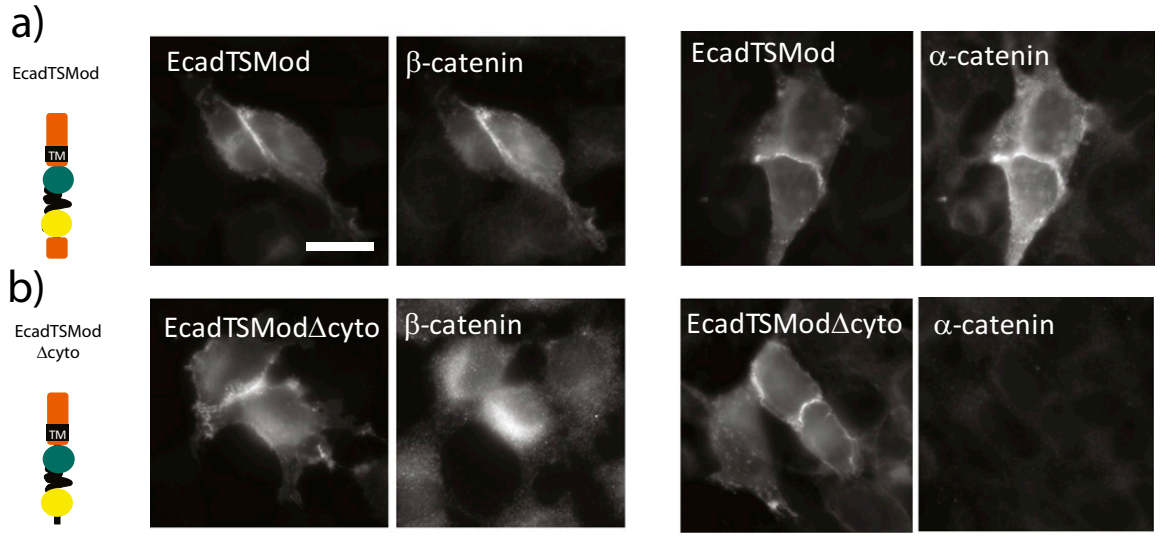

Fig. S1. L cells expressing EcadTSMod (*A*) or EcadTSModΔcyto (*B*) immunostained for β- and αE-catenin. (Scale bar: 20 μm.) Both constructs rescued cell–cell adhesion. EcadTSMod, but not EcadTSModΔcyto, recruited catenins to the membrane.

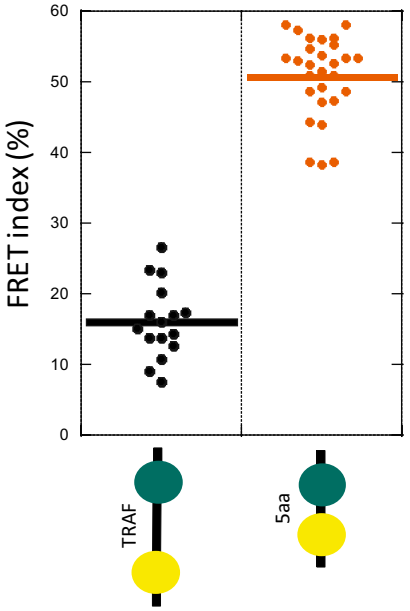

Fig. S2. FRET indices of mTFP-TRAF-Venus and mTFP-5aa-Venus in MDCK cells.

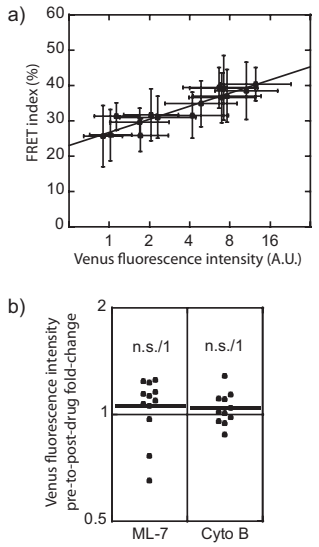

Fig. S3. (*A*) FRET index of EcadTSModΔcyto as a function of expression level (Venus intensity) in MDCK cells. Error bars show the SD of the FRET index and Venus intensity within a cell. A linear fit ($R^2 = 0.86$) in semilog$_2$ scale shows that a twofold increase in EcadTSModΔcyto expression level (surface density) leads to an increase of 3.7% ± 0.4% (SEM) in FRET index. (*B*) Venus intensity of cells expressing EcadTSMod after ML-7 or cytochalasin B treatment normalized to Venus intensity before treatment. No significant change in protein surface density occurred after drug treatment (two-tailed Mann–Whitney test).

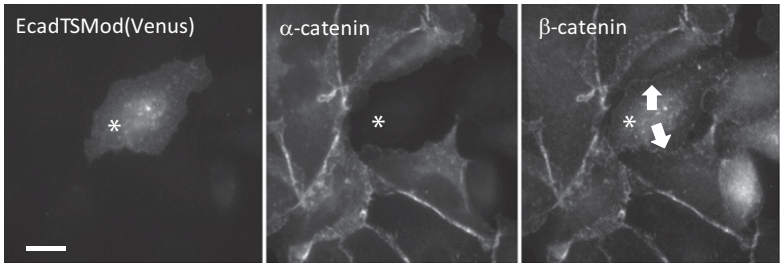

Fig. S4. MDCK cells transiently cotransfected with EcadTSMod and shRNA against αE-catenin and then immunostained for β-catenin and αE-catenin. (Scale bar: 20 μm.) Star shows cotransfected αE-catenin–depleted cell surrounded by nontransfected cells, and arrows indicate the lack of β-catenin recruitment to cell–cell contacts.

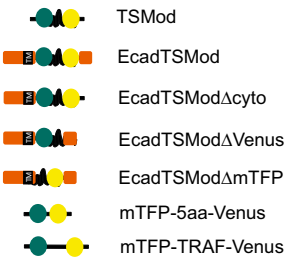

Fig. S5. Summary of the FRET constructs used in this work (see *SI Materials and Methods*, *Constructs*).